Molecular Pharmacology Fast Forward. Published on October 30, 2013 as doi:10.1124/mol.113.088633
This article has not been copyedited and formatted. The final version may differ from this version.

Title Page

Identification of overlapping, but differential binding sites for the high-affinity CXCR3 antagonists NBI-74330 and VUF11211

Danny J. Scholten, Luc Roumen, Maikel Wijtmans, Marlies C.A. Verkade-Vreeker, Hans Custers, Michael Lai, Daniela de Hooge, Meritxell Canals, Iwan J.P. de Esch, Martine J. Smit, Chris de Graaf, and Rob Leurs

Amsterdam Institute for Molecules Medicines and Systems, Division of Medicinal Chemistry, Faculty of Science, VU University Amsterdam (D.J.S, L.R., M.W., M.C.A.V., H.C., M.L., D.d.H., M.C., I.J.P.d.E., M.J.S., C.d.G., R.L.)

Molecular Pharmacology Fast Forward. Published on October 30, 2013 as DOI: 10.1124/mol.113.088633
This article has not been copyedited and formatted. The final version may differ from this version.

Running Title Page

Allosteric Antagonist Binding to the Chemokine Receptor CXCR3

Corresponding author: Rob Leurs PhD, Leiden/Amsterdam Center for Drug Research, Division of Medicinal Chemistry, Faculty of Science, VU University Amsterdam, De Boelelaan 1083, 1081 HV, Amsterdam, The Netherlands. Telephone: +31 (0) 205987579. E-mail: r.leurs@vu.nl.

Number of pages:	27
Number of tables:	2
Number of figures:	5
Number of references:	52
Number of words abstract:	245
Number of words introduction:	747
Number of words discussion:	1437

Nonstandard abbreviations:

AMG487, (R)-N-(1-(3-(4-ethoxyphenyl)-4-oxo-3,4-dihydropyrido[2,3-d]pyrimidin-2-yl)ethyl)-N-(pyridin-3-ylmethyl)-2-(4-(trifluoromethoxy)phenyl)acetamide; BSA, bovine serum albumin; CCR, CC chemokine receptor; CVX15, Arg-Arg-Nal-Cys-Tyr-Gln-Lys-dPro-Pro-Tyr-Arg-Cit-Cys-Arg-Gly-dPro; CXCL, CXC chemokine ligand; CXCR, CXC chemokine receptor; GPCR, G protein-coupled receptor; DMEM, Dulbecco's modified Eagle medium; EL, extracellular loop; ELISA, enzyme-linked immunosorbent assay; FBS, fetal bovine serum; GTPγS, guanosine 5γ-O-(3-thio)triphosphate; HEK293T, human embryonic kidney 293T cells; HIV, human immunodeficiency virus; IT1t, 1,3-dicyclohexyl-2-(3-methyl-6,6-dimethyl-5,6-dihydroimidazo[1,2-b]thiazole)-2-thiopseudourea; maraviroc, 4,4-difluoro-cyclohexanecarboxylic acid {(S)-3 [(1S,3S,5R)-3-(3-isopropyl- 5-methyl-[1,2,4]triazol-4-yl)-8-aza-bicyclo[3.2.1]oct-8-yl]-1-phenyl-propyl}-amide; NBI-74330, (R)-N-(1-(3-(4-ethoxyphenyl)-4-oxo-3,4-dihydropyrido[2,3-d]pyrimidin-2-yl)ethyl)-2-(4-fluoro-3-(trifluoromethyl)phenyl)-N-(pyridin-3-ylmethyl)acetamide; PBS, phosphate-buffered saline; PEI, polyethylene immine; PCR, polymerase chain reaction; SAR, structure-activity relationship; TBS, Tris-buffered saline; TM, transmembrane; TMS, transmembrane site; VUF11211, (S)-5-Chloro-6-(4-(1-(4-chlorobenzyl)piperidin-4-yl)-3-ethylpiperazin-1-yl)-N-ethylnicotinamide; WT, wild type;

Molecular Pharmacology Fast Forward. Published on October 30, 2013 as DOI: 10.1124/mol.113.088633
This article has not been copyedited and formatted. The final version may differ from this version.

Abstract

Chemokine receptor CXCR3 and/or its main three ligands CXCL9, CXCL10, and CXCL11 are highly upregulated in a variety of diseases. As such, considerable efforts have been made to develop small-molecule receptor CXCR3 antagonists, yielding distinct chemical classes of antagonists blocking binding and/or function of CXCR3 chemokines. Although it is suggested that these compounds bind in an allosteric fashion, so far no evidence has been provided regarding the molecular details of their interaction with CXCR3. Using site-directed mutagenesis complemented with in silico homology modeling, we report the binding modes of two high-affinity CXCR3 antagonists of distinct chemotypes: VUF11211 (piperazinyl-piperidine) with a rigid elongated structure containing two basic groups, and NBI-74330 (8-azaquinazolinone) without any basic group. Here we show that NBI-74330 is anchored in the transmembrane minor pocket lined by helices 2 (W2.60, D2.63), 3 (F3.32), and 7 (S7.39, Y7.43), whereas VUF11211 extends from the minor pocket into the major pocket of the transmembrane domains, located between residues in helices 1 (Y1.39), 2 (W2.60), 3 (F3.32), 4 (D4.60), 6 (Y6.51), and 7 (S7.39, Y7.43). Mutation of these residues did not affect CXCL11 binding significantly, confirming the allosteric nature of the interaction of these small molecules with CXCR3. Moreover, the model derived from our *in silico*-guided studies fits well with the already published structure-activity relationship data on these ligands. Altogether, in this study we show overlapping, yet different binding sites for two high-affinity CXCR3 antagonists, which offer new opportunities for the structure-based design of allosteric modulators for CXCR3.

Molecular Pharmacology Fast Forward. Published on October 30, 2013 as DOI: 10.1124/mol.113.088633
This article has not been copyedited and formatted. The final version may differ from this version.

Introduction

The chemokine system is intimately involved in leukocyte homeostasis and directing immune cells to sites of infection or inflammation (Viola and Luster, 2008). Inappropriate expression of chemokine ligands or their respective G-protein coupled receptors (GPCRs) can result in disproportionate infiltration of specific immune cells into (inflamed) tissues or confer chemokine sensitivity to cells, normally non-responsive to chemokines (O'Hayre et al., 2008). Ultimately, this leads to development of autoimmune diseases, chronic inflammation, or tumor growth and metastasis (Koelink et al., 2012). Chemokines are the endogenous peptide ligands of chemokine receptors with molecular weights of approximately 10 kDa. Chemokines are 10-50 fold larger than the average small molecule that binds these receptors. Nonetheless, many of these small ligands are able to inhibit chemokine-induced responses and/or the binding of these chemokines with nanomolar potencies (Scholten et al., 2012a). Intuitively, such size differences would suggest allosteric non-competitive mechanisms of action for small-molecule antagonists acting via distinct binding sites. In general, the interaction of chemokines with their receptors can be described by a two-step model, in which a chemokine first binds to the N-terminus of its respective GPCR. Subsequently, the N-terminus of the chemokine is positioned such that it interacts with the extracellular loops (ELs) and transmembrane (TM) domains of the GPCR. The lack of structural data on chemokine-GPCR binding hinders molecular understanding on how small molecules act at this subclass of family A GPCRs. Fortunately, structural information on chemokine receptors has started to emerge with the recent publication of chemokine receptor CXCR4 and CCR5 crystal structures (Wu et al., 2010; Tan et al., 2013), opening up new possibilities for structure-based drug design on the chemokine receptor family (Kooistra et al., 2013; Scholten et al., 2012a). In general, three pockets are distinguished in GPCRs, two in the TM domains, including the minor pocket or TM site 1 (TMS1) lined by TM helices 1 and 2, and the major pocket (transmembrane site 2 or TMS2) delimited by helices 4, 5, and 6 (figure 1A). Residues in helices 3 and 7 constitute the interface between both pockets, pointing either to one or the other pocket. Furthermore, a third pocket, lining the intracellular surface of the GPCR, was recently suggested as binding site for certain CXCR2 ligands (Nicholls et al., 2008; Salchow et al., 2010). In CXCR4, the small molecule IT1t binds in TMS1, whereas the CVX-15 peptide interacts only with residues in TMS2, showing that ligands for the same receptor can bind to different pockets in the TM domains of chemokine receptors (Wu et al., 2010).

Molecular Pharmacology Fast Forward. Published on October 30, 2013 as DOI: 10.1124/mol.113.088633
This article has not been copyedited and formatted. The final version may differ from this version.

The CXC Chemokine receptor CXCR3 is a key regulator of T-cell responses and has been linked to several diseases. Overexpression of the CXCR3 receptor and/or its ligands (CXCL9, CXCL10, CXCL11) is often observed in e.g. rheumatoid arthritis and transplant rejection (Lacotte et al., 2009). In the past decade, many efforts have focused on discovery of small molecule CXCR3 antagonists, leading to the disclosure of ligands with a multitude of different chemotypes (Wijtmans et al., 2010; Wijtmans et al., 2008). Initially, 8-azaquinazolinone compounds from Amgen (AMG487) and Neurocrine Biosciences (NBI-74330) were shown to bind CXCR3 with nanomolar affinities (Heise et al., 2005; Johnson et al., 2007; Verzijl et al., 2008), and are effective in animal models of disease (van Wanrooij et al., 2008; Walser et al., 2006). AMG487 was even assessed in clinical trials for treatment of psoriasis, but was discontinued after a phase IIa trial (Tonn et al., 2009). Moreover, a piperazinyl-piperidine compound class with high affinity CXCR3 ligands has been disclosed by Schering Plough (now Merck-Sharp & Dohme) (McGuinness et al., 2006; McGuinness et al., 2009; Shao et al., 2011). This compound series is effective in rodent models of CXCR3-associated disease, including transplant rejection and rheumatoid arthritis (Jenh et al., 2012).

Despite the interest in small-molecule antagonists for CXCR3, little information is available about their interaction with CXCR3 at the molecular level; as whether they bind to TMS1, TMS2, or both. In this study, we aimed to elucidate the binding mode of two high-affinity CXCR3 ligands from the 8-azaquinazolinone and the piperazinyl-piperidine class using site-directed mutagenesis complemented with *in silico* modeling of CXCR3. We show that NBI-74330, from the azaquinazolinone class from Amgen (figure 1) (Heise et al., 2005; Johnson et al., 2007) mainly binds to TMS1 whereas a chlorobenzyl derivative of the piperazinyl-piperidine class disclosed by Merck (McGuinness et al., 2006) with one of the highest CXCR3 affinities reported to that date (named VUF11211, figure 1) (Shao et al., 2011), binds to both TMS1 and TMS2.

Molecular Pharmacology Fast Forward. Published on October 30, 2013 as DOI: 10.1124/mol.113.088633
This article has not been copyedited and formatted. The final version may differ from this version.

Materials and methods

Materials. Dulbecco's modified Eagle's medium and trypsin were purchased from PAA Laboratories GmbH (Pasching, Austria), penicillin and streptomycin were obtained from Lonza (Verviers, Belgium), fetal bovine serum (FBS) was purchased from Integro B.V. (Dieren, The Netherlands), [^{125}I]-CXCL11 (±1000 Ci/mmol) was obtained from PerkinElmer Life and Analytical Sciences (Boston, MA, USA). Unlabeled chemokines were purchased from PeproTech (Rocky Hill, NJ, USA). Unless stated otherwise, all other chemicals were obtained from Sigma Aldrich (St. Louis, MO, USA).

CXCR3 ligands. VUF11211 (compound **18i** in (Shao et al., 2011)) was synthesized in enantiopure form in our group according to the general synthetic procedures patented by Merck (McGuinness et al., 2006). Details of the synthetic procedures are provided in the Supplemental Information (Supplemental Methods). The synthesis of NBI-74330 has been described before (Storelli et al., 2007).

DNA Constructs and Site-Directed Mutagenesis. The DNA coding for human CXCR3 was a gift from Prof Dr. B. Moser (Cardiff University School of Medicine, Cardiff, UK) and was inserted in the expression vector pcDEF$_3$. Mutants were generated by using PCR primers containing one or more mismatches in the center of the primer, flanked by 15-20 base pairs. At first, two individual polymerase chain reactions (PCRs) were performed simultaneously to amplify the first part of the receptor until the desired mutation, and the second part of the receptor from the mutation until the BGH polyA sequence. The forward primer used to generate the first part (pcDEF$_3$-FW; 5'-gggtggagactgaagttaggcc-3') recognizes part of the EF1α promoter, whereas the reverse primer for the second part (pcDEF$_3$-RV; 5'ggaaggcacgggggaggggc-3') targets part of the BGH polyA sequence of the vector. The reverse primer for the first part and forward primer for the second, are reverse complementary and recognize CXCR3 around the desired mutation as mentioned above. See the Supplemental Information for the sequences of these mutation-specific primers (Supplemental Table 1). Subsequently, a second PCR with primers pcDEF$_3$-FW and pcDEF$_3$-RV was performed to fuse both receptor DNA fragments, making use of the overlapping sequence in both individual parts as internal primer. Finally, the resulting products were digested using BamHI and XbaI restriction enzymes and ligated into pcDEF$_3$. Sequences were confirmed using Sequencing (Macrogen, Amsterdam, The Netherlands).

Molecular Pharmacology Fast Forward. Published on October 30, 2013 as DOI: 10.1124/mol.113.088633
This article has not been copyedited and formatted. The final version may differ from this version.

In Silico CXCR3 model Construction. A three-dimensional model for the CXCR3 receptor was constructed with MOE version 2011.10 (Chemical Computing Group Inc., Montreal, ON, Canada) based on the structure of CXCR4 co-crystallized with the small molecule IT1t (Protein Databank code 3ODU (Wu et al., 2010)). The primary sequence of CXCR3 (Genbank accession no. P49682) was aligned to that of the CXCR4 crystal structure. The N-terminal residues 1 to 41 were omitted from the model due to a lack of crystallographic data. An initial model was constructed for the CXCR3–VUF11211 complex as a basis for the binding model for NBI-74330. VUF11211 was docked into the model using GOLD v4 (Verdonk et al., 2003). Subsequently, protein-ligand interactions were optimized in MOE by energy minimization during which all heavy atoms were tethered with a 10.0 kcal/mol restraint, similar to the protocol our group recently described (de Kruijf et al., 2011). However, since the CXCR4–IT1t template contains lipids protruding into protein between TM5 and TM6 and the C-terminus blocking the extracellular opening (Roumen et al., 2012), the binding pocket of a CXCR3 model is spacious and VUF11211 cannot form an interaction with W268$^{6.48}$. To explain all site-directed mutagenesis data, the CXCR3 model was optimized within this region by moving TM6 by 2Å closer to TM3 and TM5, followed by the same energy minimization protocol (de Kruijf et al., 2011). This resulted in a TM arrangement comparable to that of the aminergic receptors (Shimamura et al., 2011). Using the finalized CXCR3 model, NBI-74330 was docked into the protein pocket with GOLD resulting in a pose that is in accordance with the site-directed mutagenesis data from this study, and optimized by energy minimization.

Residue numbering throughout the manuscript is displayed as absolute sequence numbers with the Ballesteros-Weinstein notation in superscript (e.g. W109$^{2.60}$). If residues are compared between different receptors, only the Ballesteros-Weinstein notation is used (e.g. W2.60) (Ballesteros and Weinstein, 1995).

Cell Culture and Transfection. HEK293T cells were grown at 37°C and 5% CO_2 in Dulbecco's modified Eagle's medium (DMEM) supplemented with 10% FBS, penicillin, and streptomycin. Cells were transfected with 2.5 ug of pcDEF$_3$-CXCR3 WT or pcDEF$_3$ containing the mutant CXCR3 DNA, and 2.5 ug of pcDEF$_3$ per 2 million cells, using linear polyethyleneimine (PEI) with a molecular weight of 25 kDa (Polysciences, Warrington, PA) as described previously (Verzijl et al., 2008).

ELISA Expression Assay. The day after transfection, cells were trypsinized, resuspended into fresh culture medium, and plated in poly-L-lysine-coated 48-well assay plates. The ELISA procedure was

Molecular Pharmacology Fast Forward. Published on October 30, 2013 as DOI: 10.1124/mol.113.088633
This article has not been copyedited and formatted. The final version may differ from this version.

performed as reported earlier (Scholten et al., 2012b). Briefly, 48 h after transfection the cells were fixed with 4% formaldehyde solution, permeabilized by 0.5% Nonidet P40 and stained with anti-CXCR3 antibody mAb160 (R&D Systems, Minneapolis, USA), and subsequently with goat anti-mouse horseradish peroxidase-conjugated antibody (BioRad Laboratories, Hercules, USA). O-phenylenediamine was used as a substrate for the enzyme coupled to the secondary antibody. The resulting color was detected using a Powerwave X340 absorbance plate reader (BioTek, Bad Friedrichshall, Germany).

Membrane Preparation. Membrane preparation was performed as described previously (Verzijl et al., 2008). In brief, cell membrane fractions from HEK293T cells, transiently transfected with WT or mutant CXCR3, were prepared by washing with ice-cold PBS. Subsequently, the cells were collected in tubes and centrifuged at 1500*g* for 10 min. The pellet was resuspended in ice-cold membrane buffer (15 mM Tris, pH 7.5, 1 mM EGTA, 0.3 mM EDTA, and 2 mM $MgCl_2$), and homogenized using a Teflon-glass homogenizer and rotor. The membranes were subjected to two freeze-thaw cycles using liquid nitrogen, and centrifuged at 40,000 *g* for 25 min. The pellet was resuspended in Tris-sucrose buffer (20 mM Tris, 250 mM sucrose, pH 7.4) and aliquots were stored at -80°C.

Radioligand Binding Assays. For [^{125}I]-CXCL11 binding, between 2 and 10 µg of membranes were used per well depending on the mutant, in 96-well clear plates (Greiner Bio One, Alphen a/d Rijn, the Netherlands). For displacement binding experiments, membranes were incubated in binding buffer (50 mM HEPES, pH 7.4, 1 mM $CaCl_2$, 5 mM $MgCl_2$, 100 mM NaCl, and 0.5% (w/v) BSA fraction V) with approximately 70 pM of [^{125}I]-CXCL11 and a concentration range of cold CXCL11, VUF11211 or NBI-74330 for 2 h at room temperature. Next, the membranes were harvested by filtration through Unifilter 96-well GF/C plates (Perkin–Elmer) presoaked with 0.5% PEI, using ice-cold wash buffer (binding buffer supplemented with 0.5M of NaCl). Bound radioactivity was determined with a MicroBeta scintillation counter (Perkin–Elmer).

Data analysis. Prism v5.0d from GraphPad software was used to plot and analyze the data.

Molecular Pharmacology Fast Forward. Published on October 30, 2013 as DOI: 10.1124/mol.113.088633
This article has not been copyedited and formatted. The final version may differ from this version.

Results

To dissect the binding modes of the two selected CXCR3 antagonists, we considered the homology between different chemokine receptors, focusing on residues that had previously been shown to be involved in the binding of small molecule antagonists to a variety of CC and CXC chemokine receptors. In figure 2 an alignment of transmembrane binding pocket residues from CC and CXC chemokine receptors is shown, with amino acid residues highlighted which affect ligand binding when mutated (de Mendonça et al., 2005; Jensen et al., 2007; Kondru et al., 2008; Vaidehi et al., 2006; Watson et al., 2005; Wong et al., 2008; Wu et al., 2010). In the next sections we will focus on specific features of the different binding pockets.

Negatively charged ligand anchors

In general, small-molecule ligands for chemokine receptors are characterized by a positively charged quaternary ammonium and aromatic groups around it (Wijtmans et al., 2008). This positive charge often contributes significantly to the affinity of the ligand, as observed for e.g. the bisaryl- and piperazinyl-piperidine class of CXCR3 ligands (Shao et al., 2011; Wijtmans et al., 2011). Calculations with Marvin tools (version 5.2.0, ChemAxon Kft, Budapest, Hungary) suggest that protonation of VUF11211 at pH 7.4 occurs at either the piperidine nitrogen (45%) or the trialkyl-nitrogen of the piperazine (43%), leaving 13% of the compound non-protonated.

As can be deduced from figure 2 a negatively charged glutamic acid at position 7.39 is highly conserved in the chemokine receptor family. This residue is often found to be the ionic anchor for a positive charge in chemokine receptor ligands, as for example for CCR1, CCR5, CXCR4, and viral chemokine receptor US28 (Casarosa et al., 2003; Kondru et al., 2008; Vaidehi et al., 2006; Wong et al., 2008). Yet, CXCR3 does not possess a negatively charged residue at this position and we therefore considered other potential anchors that could accommodate the positive charge in VUF11211. The chemokine receptor alignment in Figure 2 and the detailed information from the recently solved CXCR4 co-crystal structures, indicate that other negatively charged residues can also be involved in anchoring chemokine receptor ligands. Aspartates D2.63, D4.60 and D6.58 are e.g. involved in binding of small ligands to CXCR4 (Wong et al., 2008; Wu et al., 2010), whereas D2.63 has been shown to be involved in the binding of small molecule CXCR3 agonists (Nedjai et al., 2012). To identify the negatively charged residues in CXCR3 that act as partners for ionic interaction with the

Molecular Pharmacology Fast Forward. Published on October 30, 2013 as DOI: 10.1124/mol.113.088633
This article has not been copyedited and formatted. The final version may differ from this version.

positively charged VUF11211 we started therefore this study by mutating 10 negatively charged aspartate or glutamate residues (see Table 1); seven residing in the TM domains, one in the N-terminus close to TM1, and two in extracellular loop (EL) 2. All these residues were mutated to asparagine, thereby preventing any ionic interaction.

Human embryonic kidney (HEK293T) cells were transiently transfected with cDNA coding for the CXCR3 wild type (WT) or mutant receptors. Next, protein expression levels were determined for each mutant using a whole-cell based ELISA (Table 1). All the mutants were expressed between 68 and 121% of the level of WT CXCR3. Membranes were prepared from the transfected cells (see materials and methods), and used for competition binding experiments using [^{125}I]-CXCL11 as the radioligand (table 1). The affinity of CXCL11 for all mutants was determined to investigate the effect of the introduced mutations on CXCL11 binding. The affinity of CXCL11 was hardly affected (max only ±2 fold) by any of these mutations as shown in Table 1 (and figure 3A), with D282$^{6.62}$N as the exception. Although this mutant protein could be detected by whole-cell based ELISA (68% of the level of WT CXCR3), no [^{125}I]-CXCL11 binding to this mutant receptor could be detected, impeding further studies. Next, the ability of VUF11211 and NBI-74330 to displace [^{125}I]-CXCL11 from CXCR3 WT and mutants was determined. Only one mutant, D186$^{4.60}$N, resulted in a 10-fold decrease in affinity for VUF11211 (pIC_{50} from 7.8 to 6.8, table 1; figure 3B), where the other aspartic- and glutamic acid to asparagine mutations hardly affected the potency of VUF11211 to displace [^{125}I]-CXCL11 from the mutant CXCR3 proteins (table 1). Surprisingly, mutation of aspartic acid D112$^{2.63}$ reduced potency of NBI-74330 to displace [^{125}I]-CXCL11 binding by more than 10-fold compared to WT (pIC_{50} 7.2 to 6.1, Table 1; figure 3C) despite the absence of a positive charge in the compound.

Aromatic cages in CXCR3

Next to ionic interactions, many chemokine receptor ligands engage in interactions with hydrophobic aromatic amino acids present in the TM binding cavities of this receptor class. Figure 2 shows that many ligands appear to interact with such residues, including the conserved Y1.39 and W2.60 residues in TMS1, Y/F3.32 and F3.36 in the interface, and W6.48 and Y/F6.51 in TMS2 (Roumen et al., 2012; Scholten et al., 2012a). These conserved residues form the so-called ‘aromatic cages’ within the transmembrane region in which hydrophobic and aromatic moieties of chemokine receptor antagonist can be are positioned (Surgand et al., 2006). Examples are BX471 and UCB-35624 binding

Molecular Pharmacology Fast Forward. Published on October 30, 2013 as DOI: 10.1124/mol.113.088633
This article has not been copyedited and formatted. The final version may differ from this version.

to CCR1 (de Mendonça et al., 2005; Vaidehi et al., 2006), maraviroc and aplaviroc to CCR5 (Kondru et al., 2008; Watson et al., 2005), LMD-009 to CCR8 (Jensen et al., 2007) and AMD3100 (plerixafor) to CXCR4 (Wong et al., 2008). To study the involvement of aromatic stacking interactions in the binding of VUF11211 and NBI-74330, the aromatic phenylalanine F131$^{3.32}$ and F135$^{3.36}$ and tyrosine residues Y60$^{1.39}$, Y271$^{6.51}$, and Y308$^{7.43}$ were mutated to alanine. All mutants were expressed at levels ranging from 41% to 106% of WT CXCR3 and had no appreciable effect on the affinity of [^{125}I]-CXCL11 (Table 2). The mutation of Y271$^{6.51}$ to alanine resulted in a 7- and 10-fold reduction in affinity for NBI-74330 and VUF11211, respectively. In addition, both small ligands displayed lower affinity (8- to 30-fold) at F131$^{3.32}$A and Y308$^{7.43}$A mutants (table 2; figure 3). F131$^{3.32}$ was also mutated to a histidine residue (which is present at position 3.32 in CXCR5, see figure 2) to investigate the possibility of aromatic interactions between the ligands and a different type of aromatic ring. This mutant was comparable to WT with respect to [^{125}I]-CXCL11 binding affinity, and only resulted in very minor decreases in affinity for VUF11211 and NBI-74330.

In chemokine receptors, W109$^{2.60}$ is a highly conserved tryptophan residue (figure 2) close to the TxP motif (Govaerts et al., 2001), indicating that it is important for chemokine receptor stability and function, and W268$^{6.48}$ has been hypothesized as important for receptor function for numerous GPCRs (Elling et al., 2006; Schwartz et al., 2006). Several chemokine receptors feature a glutamine residue at these positions which is similar in size to a tryptophan, yet lacks aromaticity (figure 2). Therefore, W109$^{2.60}$ and W268$^{6.48}$ were selected for mutation to a glutamine. These mutant proteins were expressed at 81% and 60% compared to WT levels, respectively. Moreover, affinity of [^{125}I]-CXCL11 was unaltered at these mutants. The W268$^{6.48}$Q mutation lowered the binding affinity of only VUF11211 (6-fold; pIC_{50} from 7.8 to 7.0; table 2). Yet, the W109$^{2.60}$ residue appears to be very important for the binding of both NBI-74330 as well as VUF11211, as its mutation to glutamine led to a 500- and 630-fold decrease in affinity for NBI-74330 and VUF11211, respectively. (table 2; figure 3).

Hydrogen bonding

Next to aromatic stacking, also opportunities exist for the ligands to engage in hydrogen bonding with residues in the TM domains. As such, the serine (S301$^{7.36}$ and S304$^{7.39}$) and tyrosine residues (Y60$^{1.39}$ and Y308$^{7.43}$) were mutated to non-hydroxylated amino acids (alanine and phenylalanine, respectively) to investigate involvement of potential hydrogen bonding with VUF11211 and NBI-74330. All mutants

Molecular Pharmacology Fast Forward. Published on October 30, 2013 as DOI: 10.1124/mol.113.088633
This article has not been copyedited and formatted. The final version may differ from this version.

showed expressions similar to WT levels (table 2). None of these mutations had a significant effect on potency of both NBI-74330 and VUF11211 to displace [^{125}I]-CXCL11, while the affinity of CXCL11 decreased 5-fold for only the S304$^{7.39}$A mutant (table 2).

The lack of significant effects on binding of NBI-74330 or VUF11211 by testing these individual mutations might be the result of possible hydrogen bonding networks between CXCR3 and the ligands. As a consequence, other residues in the vicinity might compensate for the loss of a single hydrogen bond interaction. Therefore, a triple mutant of residues in close proximity to each other in our CXCR3 homology model, namely Y60$^{1.39}$F/S304$^{7.39}$A/Y308$^{7.43}$F, was constructed. The triple mutation had no effect on [^{125}I]-CXCL11 binding, but caused a 10-fold decrease in affinity of VUF11211, suggestive of a hydrogen-bonding network for this CXCR3 antagonist. For NBI-74330 no significant decrease in affinity was observed (table 2).

Additional CXCR3 mutations

For several residues, additional mutants were constructed to investigate specific interactions. G128$^{3.29}$ is a variable residue among chemokine receptors indicating a location potentially important for selectivity between chemokine receptors. In addition, CXCR4 contains a histidine residue at this position, important for interaction with both IT1t and CVX-15 ligands (Wu et al., 2010). Moreover, introduction of a histidine at this position (G128$^{3.29}$H) in CXCR3 anchored small metal chelators to the receptor (Rosenkilde et al., 2007). As histidine is greater in size than glycine, the residue at this position was mutated to a histidine (G128$^{3.29}$H) in analogy with CXCR4, to investigate the allowed space around this residue. This mutant was well expressed in HEK293T cells (80% of WT). Interestingly, radioligand displacement potencies of CXCL11, NBI74330, and VUF11211 were all affected by this mutation, by 5, 100, or 800 fold, respectively (table 2), indicating that the larger histidine likely introduces a steric clash within the binding pocket of CXCR3 affecting the binding of all the ligands under investigation.

Finally, residue S304$^{7.39}$ was given special attention due to its analogous residue E7.39 which is relatively conserved in the chemokine receptor family and often involved in binding of small molecules (figure 2). Moreover, in CXCR4 the E7.39 interacts with the small-molecule antagonist IT1t compound in CXCR4 co-crystallized with this compound. In CXCR3, the S304$^{7.39}$ was mutated to a glutamic acid

Molecular Pharmacology Fast Forward. Published on October 30, 2013 as DOI: 10.1124/mol.113.088633
This article has not been copyedited and formatted. The final version may differ from this version.

residue to investigate the influence of a larger polar residue in the center of the protein cavity and also a leucine mutation (S304$^{7.39}$L) was included to determine whether this influence was due to the polarity or due to the size of the residue. Both mutants were expressed to a similar extent as WT, and also bind CXCL11 with similar affinity. The S304$^{7.39}$L mutation resulted in decreased potency to displace [^{125}I]-CXCL11 by 8-, or 20-fold for NBI-74330 and VUF11211, respectively (table 2). The presence of the glutamic acid at the same position was tolerated for VUF11211, but not for NBI-74330 for which a loss in affinity of 80-fold was observed.

Molecular Pharmacology Fast Forward. Published on October 30, 2013 as DOI: 10.1124/mol.113.088633
This article has not been copyedited and formatted. The final version may differ from this version.

Discussion

To rationalize the effects of CXCR3 mutations on CXCL11, NBI-74330 and VUF11211 binding (figure 4), a CXCR3 homology model was constructed based on CXCR4 co-crystallized with ligand IT1t in the TMS1 and CVX-15 in TMS2 (Surgand et al., 2006; Wu et al., 2010). The obtained site-directed mutagenesis data was used to guide the docking of NBI-74330 and VUF11211 into the homology model of CXCR3, and the models were fine-tuned by literature SAR data on both chemical series (figure 4).

Proposed binding mode of VUF11211

Binding of VUF11211 to CXCR3 is affected by several mutations introduced in the TM domains, while binding of the endogenous agonist CXCL11 is largely unchanged. In addition, displacement of a radiolabeled variant of VUF11211 by CXCL11 was incomplete (Scholten et al., unpublished observations). Moreover, a closely-related compound (SCH-546738) exhibited non-competitive antagonistic behavior on CXCL11-mediated receptor activity (Jenh et al., 2012). Overall, these findings indicate that VUF11211 affects the binding of CXCL11 to CXCR3 in an allosteric fashion.

Our CXCR3 mutation data and homology modeling studies indicate that VUF11211 interacts with residues in both TMS1 and TMS2 pockets (Figure 4A,C,E). We hypothesize that D186$^{4.60}$ serves as the anchor for the positive charge at the piperidine nitrogen of VUF11211, since a 10-fold drop in affinity was observed at the D186$^{4.60}$N mutant (table 1; figure 4A). This hypothesis is supported by SAR studies that highlight the importance of the basicity of the piperidine ring (figure 4A) (Shao et al., 2011). Rigidification of the benzyl moiety either by ring closure or intramolecular hydrogen bonding, at the cost of basicity, could maintain ligand affinity, indicating the importance of directionality for the chlorobenzyl moiety (Kim et al., 2011; Shao et al., 2011). In the proposed binding mode, the chlorobenzyl moiety resides in a small space between TM4 and TM5 (figure 4A,C,E). The importance of the S-ethyl moiety on the piperazine core was proven by various substitutions that showed a preference for a small apolar group over larger or polar moieties (McGuinness et al., 2009; Shao et al., 2011). This implies that rotation of the pyridine and the piperidine rings with respect to the piperazine ring are restricted, and in addition, that there is limited space around the ethyl moiety. In our model the piperazine moiety is close to TM6 and the finding that W268$^{6.48}$Q and Y271$^{6.51}$A mutants decrease affinity for VUF11211 7-fold and 10-fold, respectively, emphasizes the size and shape limitation of the

Molecular Pharmacology Fast Forward. Published on October 30, 2013 as DOI: 10.1124/mol.113.088633
This article has not been copyedited and formatted. The final version may differ from this version.

pocket by TM6. The loss of affinity at mutants W109$^{2.60}$Q (>600-fold, aromatic interaction), G128$^{3.29}$H (±800-fold, space), and F131$^{3.32}$A (20-fold, aromatic interaction) indicate a specific fit of the pyridyl moiety in the binding pocket of CXCR3 (figure 4A,C,E). Finally, modification of the amide moiety by removal or repositioning of the nitrogen atom indicated a role for hydrogen bonding of the nitrogen atom (±10-fold difference in affinity) (McGuinness et al., 2009; Shao et al., 2011). Removal of the hydroxyl moiety from the residues Y60$^{1.39}$, S304$^{7.39}$ or Y308$^{7.43}$ showed that none of them specifically formed an interaction with the amide moiety of VUF11211. Since the triple mutation (Y60$^{1.39}$F/S304$^{7.39}$A/Y308$^{7.43}$F) showed a 10-fold reduction in affinity, we suggest that at least these three residues that are in close proximity to VUF11211 and might form a hydrogen-bonding network within the CXCR3 binding pocket (figure 4A,C). Apparently, these amino acid residues are able to compensate for the removal of the hydrogen-bonding capabilities of a nearby residue. The involvement of hydrogen bonding is also indicated by mutation of S304$^{7.39}$ to glutamic acid or leucine. The results obtained with the S304$^{7.39}$E mutant show that a hydrogen bond acceptor moiety (i.e. the alcohol oxygen in S340$^{7.39}$ or carboxylate oxygen atoms in E304$^{7.39}$) is required, which is proposed to interact with the amide moiety. However, the introduction of a large hydrophobic group with S304$^{7.39}$L reduces the affinity of VUF11211 by 20-fold.

Binding hypothesis of NBI-74330

Multiple mutations affected the binding of NBI-74330, whereas CXCL11 affinity remained unchanged. Furthermore, NBI-74330 exhibited non-competitive insurmountable antagonism in various functional assays, including phospholipase C activation (Heise et al., 2005; Verzijl et al., 2008). In addition, CXCL11 could not completely displace the radiolabeled closely-related NBI-74330 analogue RAMX3 (Bernat et al., 2012). Altogether, these pharmacological data combined with our *in-silico* guided mutagenesis studies suggest an allosteric mode of action for NBI-74330.

Since NBI-74330 does not possess highly basic moieties and hence lacks H-bond donor atoms, the reduction of affinity observed at the D112$^{2.63}$N mutant is remarkable (table 1; figure 3C). The quinazolinone nitrogen atoms and associated positive partial charge on the 7-position of the ring is important for CXCR3 antagonism (Johnson et al., 2007; Liu et al., 2009; Storelli et al., 2007). As such, we propose that an aromatic -CH group of the 8-azaquinazolinone moiety of NBI-74330 forms a weak hydrogen bond to D112$^{2.63}$, like N-heteroaromatic -CH groups in pyridine (Balevicius et al., 2007) and

Molecular Pharmacology Fast Forward. Published on October 30, 2013 as DOI: 10.1124/mol.113.088633
This article has not been copyedited and formatted. The final version may differ from this version.

quinolin-8-ol (Zhang et al., 2013) rings (figure 4D,F). The ligand SAR and CXCR3 mutagenesis data however do not exclude indirect water-mediated H-bond interactions between the pyridine nitrogen and the carboxylate group of D112$^{2.63}$, like the water-mediated H-bond network between the tetrazole moiety of maraviroc and the hydroxyl group of Y1.39 in the CCR5 crystal structure (figure 5C) (Tan et al., 2013). In the proposed binding mode the quinazolinone ring stacks with W109$^{2.60}$, which is corroborated by the site-directed mutagenesis data (500-fold reduction in NBI-74330 affinity at the W109$^{2.60}$Q mutant). The ethoxy-phenyl moiety is located close to TM3, in line with the 100-fold reduction of NBI-74330 affinity at G128$^{3.29}$H mutant, likely due to a steric clash in the mutant receptor (figure 4D,F).

The electron-withdrawing character of the trifluoromethyl moiety is also an important determinant for ligand affinity (>100-fold better over unsubstituted benzyl) (Storelli et al., 2005; Storelli et al., 2007). Polar aromatic interactions between CXCR3 and NBI-74330 are identified by F131$^{3.32}$A, Y271$^{6.51}$A and Y308$^{7.43}$A, reducing affinity by 10-fold, 6-fold and 30-fold, respectively (table 2; figure 4B,D,F). Substitution of the serine at position 304$^{7.39}$ by a glutamic acid showed a large reduction in affinity (80-fold), which is mainly caused by the increased hydrophobicity (20-fold reduction in the case of S304$^{7.39}$L).

CXCR3 antagonist binding pockets

Different mutations in the TM region impacted NBI-74330 or VUF11211 binding, yet did not significantly affect CXCL11 affinity (figure 3), suggesting that CXCL11 does not bind to the TM domains (Xanthou et al., 2003; Trotta et al., 2009) and that these small molecules are allosteric CXCR3 ligands. However, chemokines are considerably larger, and most of their interaction energy comes from binding to the N-terminus and ELs of the receptor. A small part of the chemokine (N-terminus) is thought to interact with the receptor TM bundle for receptor activation. As such, potential overlap in interacting residues of the CXCR3 N-terminus and small molecules in TMS1/2 cannot be ruled out at this point.

Interestingly, and similar to CXCR2 and CXCR4, these ligands bind differentially in the TM pockets within CXCR3. In our homology model of CXCR3, NBI-74330 binds mainly to TMS1 residues (figure 5A), as also observed for the antagonist IT1t co-crystallized with the CXCR4 receptor (Wu et al., 2010) (figure 5B: cyan, versus figure 5A: magenta). NBI-74330 seems to span TMS2 to a small extent,

Molecular Pharmacology Fast Forward. Published on October 30, 2013 as DOI: 10.1124/mol.113.088633
This article has not been copyedited and formatted. The final version may differ from this version.

where only the Y271$^{6.51}$A affected its binding affinity (6-fold). The TMS1 binding pocket has also been identified for ligands in other chemokine receptors, e.g. UCB-35625 in CCR1 (Y1.39, Y3.32 and E7.39) (de Mendonça et al., 2005), LMD-009 in CCR8 (Y1.39, Q2.60, S3.29, Y3.32 and E7.39) (Jensen et al., 2007), and IT1t in CXCR4 (D2.63 and E7.39) (Wu et al., 2010). On the other hand, VUF11211 with its elongated shape is anchored in TMS1 and traverses TMS2 to a much larger degree than NBI-74330, interacting with residues including W109$^{2.60}$, F131$^{3.32}$, D186$^{4.60}$, and Y271$^{6.51}$ (figure 5A). Interestingly, in a recent CCR5 crystal structure maraviroc also binds in both pockets (e.g. Y1.39, W2.60, Y3.32, W6.48, Y6.51, I5.42, E7.39) (Tan et al., 2013) (figure 5**C**), whereas in a CXCR4 crystal structure, the CVX-15 peptide exclusively binds to TMS2 (figure 5B) (Wu et al., 2010). The relatively large CVX-15 peptide stretches out to the extracellular loops (figure 5B), while VUF11211 seems to bind in a more horizontal fashion (figure 5A). Ligands for other chemokine receptors also stretch both binding pockets, e.g. BX-471 in CCR1 (Y1.39, Y3.33, I6.55, Y7.43) (Vaidehi et al., 2006), and AMD3100 in CXCR4 (Y1.39, W2.60, Y3.32, D4.60, D6.58, E7.39) (Wong et al., 2008; Wu et al., 2010). In conclusion, in this study we report for the first time the molecular details of the binding of two high-affinity CXCR3 antagonists of distinct chemotypes. Fundamental knowledge on ligand interactions with the CXCR3 receptor may fuel the structure-based design and optimization of CXCR3 ligands in the future.

Acknowledgments

We thank Elwin Janssen for technical assistance in the determination of optical purities.

Authorship Contributions

Participated in research design: Scholten, Roumen, Vreeker, Wijtmans, Custers, Lai, de Hooge, Canals, de Esch, Smit, de Graaf, Leurs

Conducted experiments: Scholten, Roumen, Wijtmans, Vreeker, Custers, Lai, de Hooge, Canals, de Graaf

Contributed new reagents or analytic tools: Wijtmans, Custers, Lai, de Esch, de Graaf

Performed data analysis: Scholten, Roumen, Vreeker, Wijtmans, Custers, de Hooge, Canals, Smit, de Graaf, Leurs

Molecular Pharmacology Fast Forward. Published on October 30, 2013 as DOI: 10.1124/mol.113.088633
This article has not been copyedited and formatted. The final version may differ from this version.

Wrote or contributed to the writing of the manuscript: Scholten, Roumen, Wijtmans, Smit, de Graaf, Leurs

References

Balevicius V, Bariseviciute R, Aidas K, Svoboda I, Ehrenberg H, and Fuess H (2007) Proton transfer in hydrogen-bonded pyridine/acid systems: the role of higher aggregation. Phys Chem Chem Phys 9(24):3181-3189.

Ballesteros JA and Weinstein H (1995) Integrated methods for the construction of three-dimensional models and computational probing of structure-function relations in G protein-coupled receptors, in *Receptor Molecular Biology* (Sealfon SC ed) vol. 25: pp 366-428, Academic Press.

Bernat V, Heinrich MR, Baumeister P, Buschauer A, and Tschammer N (2012) Synthesis and Application of the First Radioligand Targeting the Allosteric Binding Pocket of Chemokine Receptor CXCR3. ChemMedChem 7(8):1481–1489.

Casarosa P, Menge WM, Minisini R, Otto C, van Heteren J, Jongejan A, Timmerman H, Moepps B, Kirchhoff F, Mertens T, Smit MJ, and Leurs R (2003) Identification of the first nonpeptidergic inverse agonist for a constitutively active viral-encoded G protein-coupled receptor. J Biol Chem 278(7):5172-5178.

de Graaf C, Foata N, Engkvist O, and Rognan D (2008) Molecular modeling of the second extracellular loop of G-protein coupled receptors and its implication on structure-based virtual screening. Proteins 71(2):599-620.

de Kruijf P, Lim HD, Roumen L, Renjaän VA, Zhao J, Webb ML, Auld DS, Wijkmans JCHM, Zaman GJR, Smit MJ, de Graaf C, and Leurs R (2011) Identification of a novel allosteric binding site in the CXCR2 chemokine receptor. Mol Pharmacol 80(6):1108–1118.

de Mendonça F, da Fonseca P, Phillips R, Saldanha J, Williams T, and Pease J (2005) Site-directed mutagenesis of CC chemokine receptor 1 reveals the mechanism of action of UCB 35625, a small molecule chemokine receptor antagonist. J Biol Chem 280(6):4808-4816.

Elling CE, Frimurer TM, Gerlach LO, Jorgensen R, Holst B, and Schwartz TW (2006) Metal ion site engineering indicates a global toggle switch model for seven-transmembrane receptor activation. J Biol Chem 281(25):17337-17346.

Govaerts C, Blanpain C, Deupi X, Ballet S, Ballesteros J, Wodak S, Vassart G, Pardo L, and Parmentier M (2001) The TXP motif in the second transmembrane helix of CCR5. A structural determinant of chemokine-induced activation. J Biol Chem 276(16):13217-13225.

Heise CE, Pahuja A, Hudson SC, Mistry MS, Putnam AL, Gross MM, Gottlieb PA, Wade WS, Kiankarimi M, Schwarz D, Crowe P, Zlotnik A, and Alleva DG (2005) Pharmacological characterization of CXC chemokine receptor 3 ligands and a small molecule antagonist. J Pharmacol Exp Ther 313(3):1263-1271.

Jenh CH, Cox MA, Cui L, Reich EP, Sullivan L, Chen SC, Kinsley D, Qian S, Kim SH, Rosenblum S, Kozlowski J, Fine JS, Zavodny PJ, and Lundell D (2012) A selective and potent CXCR3 antagonist SCH 546738 attenuates the development of autoimmune diseases and delays graft rejection. BMC Immunol 13(1):2.

Jensen PC, Nygaard R, Thiele S, Elder A, Zhu G, Kolbeck R, Ghosh S, Schwartz TW, and Rosenkilde MM (2007) Molecular interaction of a potent nonpeptide agonist with the chemokine receptor CCR8. Mol Pharmacol 72(2):327-340.

Johnson M, Li AR, Liu J, Fu Z, Zhu L, Miao S, Wang X, Xu Q, Huang A, Marcus A, Xu F, Ebsworth K, Sablan E, Danao J, Kumer J, Dairaghi D, Lawrence C, Sullivan T, Tonn G, Schall T, Collins T, and Medina J (2007) Discovery and optimization of a series of quinazolinone-derived antagonists of CXCR3. Bioorg Med Chem Lett 17(12):3339-3343.

Kim SH, Anilkumar GN, Zawacki LG, Zeng Q, Yang DY, Shao Y, Dong G, Xu X, Yu W, Jiang Y, Jenh CH, Hall JW, 3rd, Carroll CD, Hobbs DW, Baldwin JJ, McGuinness BF, Rosenblum SB, Kozlowski JA, Shankar BB, and Shih NY (2011) III. Identification of novel CXCR3 chemokine receptor antagonists with a pyrazinyl-piperazinyl-piperidine scaffold. Bioorg Med Chem Lett 21(23):6982-6986.

Koelink PJ, Overbeek SA, Braber S, de Kruijf P, Folkerts G, Smit MJ, and Kraneveld AD (2012) Targeting chemokine receptors in chronic inflammatory diseases: an extensive review. Pharmacol Ther 133(1):1-18.

Kondru R, Zhang J, Ji C, Mirzadegan T, Rotstein D, Sankuratri S, and Dioszegi M (2008) Molecular interactions of CCR5 with major classes of small-molecule anti-HIV CCR5 antagonists. Mol Pharmacol 73(3):789-800.

Kooistra AJ, Roumen L, Leurs R, de Esch IJ, and de Graaf C (2013) From heptahelical bundle to hits from the Haystack: structure-based virtual screening for GPCR ligands. Methods Enzymol 522:279-336.

Lacotte S, Brun S, Muller S, and Dumortier H (2009) CXCR3, inflammation, and autoimmune Diseases. Ann N Y Acad Sci 1173:310-317.

Liu J, Fu Z, Li AR, Johnson M, Zhu L, Marcus A, Danao J, Sullivan T, Tonn G, Collins T, and Medina J (2009) Optimization of a series of quinazolinone-derived antagonists of CXCR3. Bioorg Med Chem Lett 19(17):5114-5118.

McGuinness BF, Carroll CD, Zawacki LG, Dong G, Yang C, Hobbs DW, Jacob-Samuel B, Hall JW 3rd, Jenh CH, Kozlowski JA, Anilkumar GN, and Rosenblum SB (2009) Novel CXCR3 antagonists with a piperazinyl-piperidine core. Bioorg Med Chem Lett 19(17):5205-5208.

McGuinness BF, Rosenblum SF, Kozlowksi JA, Anilkumar GN, Kim SH, Shih N-Y, Jenh C-H, Zavodny PJ, Hobbs DW, Dong G, Shao Y, Zawacki LG, Yang C, and Carroll CD (2006). Pyridyl and phenyl substituted piperazine-piperidines with CXCR3 antagonist activity. WO Patent 2006088919.

Nedjai B, Li H, Stroke IL, Wise EL, Webb ML, Merritt JR, Henderson I, Klon AE, Cole AG, Horuk R, Vaidehi N, and Pease JE (2012) Small molecule chemokine mimetics suggest a molecular basis for the observation that CXCL10 and CXCL11 are allosteric ligands of CXCR3. Br J Pharmacol 166(3):912-923.

Nicholls DJ, Tomkinson NP, Wiley KE, Brammall A, Bowers L, Grahames C, Gaw A, Meghani P, Shelton P, Wright TJ, and Mallinder PR (2008) Identification of a putative intracellular allosteric antagonist binding-site in the CXC chemokine receptors 1 and 2. Mol Pharmacol 74(5):1193-1202.

O'Hayre M, Salanga CL, Handel TM, and Allen SJ (2008) Chemokines and cancer: migration, intracellular signalling and intercellular communication in the microenvironment. Biochem J 409(3):635-649.

Rosenkilde MM, Andersen M, Nygaard R, Frimurer TM, and Schwartz TW (2007) Activation of the CXCR3 chemokine receptor through anchoring of a small molecule chelator ligand between TM-III, -IV, and -VI. Mol Pharmacol 71(3):930-941.

Roumen L, Scholten DJ, de Kruijf P, de Esch IJP, Leurs R, and de Graaf C (2012) C(X)CR in silico: Computer-aided prediction of chemokine receptor-ligand interactions. Drug Discov Today Technol 9(4):e281-e291.

Salchow K, Bond ME, Evans SC, Press NJ, Charlton SJ, Hunt PA, and Bradley ME (2010) A common intracellular allosteric binding site for antagonists of the CXCR2 receptor. Br J Pharmacol 159(7):1429-1439.

Scholten DJ, Canals M, Maussang D, Roumen L, Smit MJ, Wijtmans M, de Graaf C, Vischer HF, and Leurs R (2012a) Pharmacological modulation of chemokine receptor function. Br J Pharmacol 165(6):1617-1643.

Scholten DJ, Canals M, Wijtmans M, de Munnik SM, Nguyen P, Verzijl D, de Esch IJP, Vischer HF, Smit MJ, and Leurs R (2012b) Pharmacological characterisation of a small-molecule agonist for the chemokine receptor CXCR3. Br J Pharmacol 166:898-911.

Schwartz TW, Frimurer TM, Holst B, Rosenkilde MM, and Elling CE (2006) Molecular mechanism of 7TM receptor activation--a global toggle switch model. Annu Rev Pharmacol Toxicol 46:481-519.

Shao Y, Anilkumar GN, Carroll CD, Dong G, Hall JW, 3rd, Hobbs DW, Jiang Y, Jenh CH, Kim SH, Kozlowski JA, McGuinness BF, Rosenblum SB, Schulman I, Shih NY, Shu Y, Wong MK, Yu W, Zawacki LG, and Zeng Q (2011) II. SAR studies of pyridyl-piperazinyl-piperidine derivatives as CXCR3 chemokine antagonists. Bioorg Med Chem Lett 21(5):1527-1531.

Shimamura T, Shiroishi M, Weyand S, Tsujimoto H, Winter G, Katritch V, Abagyan R, Cherezov V, Liu W, Han GW, Kobayashi T, Stevens RC, and Iwata S (2011) Structure of the human histamine H1 receptor complex with doxepin. Nature 475(7354):65-70.

Storelli S, Verdijk P, Verzijl D, Timmerman H, van de Stolpe AC, Tensen CP, Smit MJ, De Esch IJP, and Leurs R (2005) Synthesis and structure-activity relationship of 3-phenyl-3H-quinazolin-4-one derivatives as CXCR3 chemokine receptor antagonists. Bioorg Med Chem Lett 15(11):2910-2913.

Storelli S, Verzijl D, Al-Badie J, Elders N, Bosch L, Timmerman H, Smit MJ, De Esch IJP, and Leurs R (2007) Synthesis and structure-activity relationships of 3H-quinazolin-4-ones and 3H-pyrido[2,3-d]pyrimidin-4-ones as CXCR3 receptor antagonists. Arch Pharm (Weinheim) 340(6):281-291.

Surgand J-S, Rodrigo J, Kellenberger E, and Rognan D (2006) A chemogenomic analysis of the transmembrane binding cavity of human G-protein-coupled receptors. Proteins 62(2):509-538.

Tan Q, Zhu Y, Li J, Chen Z, Han GW, Kufareva I, Li T, Ma L, Fenalti G, Li J, Zhang W, Xie X, Yang H, Jiang H, Cherezov V, Liu H, Stevens RC, Zhao Q, and Wu B (2013) Structure of the CCR5 chemokine receptor-HIV entry inhibitor maraviroc complex. science 341(6152):1387-90.

Tonn GR, Wong SG, Wong SC, Johnson MG, Ma J, Cho R, Floren LC, Kersey K, Berry K, Marcus AP, Wang X, Van Lengerich B, Medina JC, Pearson PG, and Wong BK (2009) An inhibitory metabolite leads to dose- and time-dependent pharmacokinetics of (R)-N-{1-[3-(4-ethoxy-phenyl)-4-oxo-3,4-dihydro-pyrido[2,3-d]pyrimidin-2-yl]-ethyl}-N-pyridin-3-yl-methyl-2-(4-trifluoromethoxy-phenyl)-acetamide (AMG487) in human subjects after multiple dosing. Drug Metab Dispos 37(3):502-513.

Trotta T, Costantini S, and Colonna G (2009) Modelling of the membrane receptor CXCR3 and its complexes with CXCL9, CXCL10 and CXCL11 chemokines: Putative target for new drug design. Mol Immunol 47(2–3):332–339.

Vaidehi N, Schlyer S, Trabanino R, Floriano W, Abrol R, Sharma S, Kochanny M, Koovakat S, Dunning L, Liang M, Fox J, de Mendonca F, Pease J, Goddard W, and Horuk R (2006) Predictions of CCR1 chemokine receptor structure and BX 471 antagonist binding followed by experimental validation. J Biol Chem 281(37):27613-27620.

van Wanrooij EJ, de Jager SC, van Es T, de Vos P, Birch HL, Owen DA, Watson RJ, Biessen EA, Chapman GA, van Berkel TJ, and Kuiper J (2008) CXCR3 antagonist NBI-74330 attenuates atherosclerotic plaque formation in LDL receptor-deficient mice. Arterioscler Thromb Vasc Biol 28(2):251-257.

Verdonk ML, Cole JC, Hartshorn MJ, Murray CW, and Taylor RD (2003) Improved protein-ligand docking using GOLD. Proteins 52(4):609-623.

Verzijl D, Storelli S, Scholten DJ, Bosch L, Reinhart TA, Streblow DN, Tensen CP, Fitzsimons CP, Zaman GJ, Pease JE, de Esch IJP, Smit MJ, and Leurs R (2008) Noncompetitive antagonism and inverse agonism as mechanism of action of nonpeptidergic antagonists at primate and rodent CXCR3 chemokine receptors. J Pharmacol Exp Ther 325(2):544-555.

Viola A and Luster AD (2008) Chemokines and Their Receptors: Drug Targets in Immunity and Inflammation. Annu Rev Pharmacol Toxicol 48:171-197.

Walser TC, Rifat S, Ma X, Kundu N, Ward C, Goloubeva O, Johnson MG, Medina JC, Collins TL, and Fulton AM (2006) Antagonism of CXCR3 inhibits lung metastasis in a murine model of metastatic breast cancer. Cancer Res 66(15):7701-7707.

Watson C, Jenkinson S, Kazmierski W, and Kenakin T (2005) The CCR5 receptor-based mechanism of action of 873140, a potent allosteric noncompetitive HIV entry inhibitor. Mol Pharmacol 67(4):1268-1282.

Wijtmans M, de Esch IJP, and Leurs R (2010) Therapeutic Targeting of the CXCR3 Receptor, in *Chemokine Receptors as Drug Targets* (Smit MJ, Lira SA, and Leurs R eds) pp 301-322, Wiley-VCH Verlag GmbH & Co. KGaA, Weinheim.

Wijtmans M, Verzijl D, Bergmans S, Lai M, Bosch L, Smit MJ, de Esch IJP, and Leurs R (2011) CXCR3 antagonists: quaternary ammonium salts equipped with biphenyl- and polycycloaliphaticanchors. Bioorg Med Chem 19(11):3384-3393.

Wijtmans M, Verzijl D, Leurs R, de Esch IJP, and Smit MJ (2008) Towards small-molecule CXCR3 ligands with clinical potential. ChemMedChem 3(6):861-872.

Wong RSY, Bodart V, Metz M, Labrecque J, Bridger G, and Fricker SP (2008) Comparison of the potential multiple binding modes of bicyclam, monocylam, and noncyclam small-molecule CXC chemokine receptor 4 inhibitors. Mol Pharmacol 74(6):1485-1495.

Wu B, Chien EY, Mol CD, Fenalti G, Liu W, Katritch V, Abagyan R, Brooun A, Wells P, Bi FC, Hamel DJ, Kuhn P, Handel TM, Cherezov V, and Stevens RC (2010) Structures of the CXCR4 chemokine GPCR with small-molecule and cyclic peptide antagonists. Science 330(6007):1066-1071.

Xanthou G, Williams T, and Pease J (2003) Molecular characterization of the chemokine receptor CXCR3: evidence for the involvement of distinct extracellular domains in a multi-step model of ligand binding and receptor activation. Eur J Immunol 33(10):2927–2936.

Zhang J, Chen P, Yuan B, Ji W, Cheng Z, and Qiu X (2013) Real-Space identification of intermolecular bonding with atomic force microscopy. Science doi:10.1126/science.1242603

Molecular Pharmacology Fast Forward. Published on October 30, 2013 as DOI: 10.1124/mol.113.088633
This article has not been copyedited and formatted. The final version may differ from this version.

Footnotes

This research was performed within the framework of the Dutch Top Institute Pharma GPCR forum [project D1-105] and was financially supported by the Netherlands Organization for Scientific Research (NWO) through a VENI grant to C.d.G [Grant 700.59.408].

D.J.S., M.W., I.J.P.d.E., M.J.S., C.d.G., and R.L. participate in the European COST Action CM1207 (GLISTEN).

D.J.S. and L.R. contributed equally to this work.

M.C. Current affiliation: Drug Discovery Biology & Department of Pharmacology, Monash Institute of Pharmaceutical Sciences, Monash University, Parkville, Victoria, Australia.

Molecular Pharmacology Fast Forward. Published on October 30, 2013 as DOI: 10.1124/mol.113.088633
This article has not been copyedited and formatted. The final version may differ from this version.

Figure Legends

Figure 1.

Chemical structures of CXCR3 antagonists used in this study and a helical wheel representation of the transmembrane domains of CXCR3 with TM site 1 (TMS1) and TM site 2 (TMS2) generally involved in binding of small ligands to chemokine receptors. Residues from TM3 and TM7 constitute the interface between both pockets (see also figure 2).

Figure 2

Alignment of residues in the binding pockets of chemokine receptors. Residue numbers are in Ballesteros-Weinstein notation. Amino acids residing in the minor pocket (TMS1), major pocket (TMS2) or interface, are indicated in blue, orange and gray, respectively. The Ballesteros-Weinstein residue numbers (Ballesteros and Weinstein, 1995) are used to enumerate residues in transmembrane (TM) helices, whereas the numbering scheme proposed by de Graaf and coworkers (de Graaf et al., 2008) is used to enumerate the conserved cysteine residue (45.50) and the residue downstream from this cysteine residue (45.51) in the second extracellular loop two (EL2). Residues are colored per receptor when mutation of that particular residue is reported to affect ligand affinity or antagonism. For CCR5 and CXCR4 interactions with small molecules suggested by mutagenesis and computational modeling studies are shown in the first row, while the second row highlights residues that make contact with ligands in their respective crystal structures: maraviroc for CCR5 and IT1t and CVX15 for CXCR4. Interacting residues from these crystal structures are indicated with bold black borders. Residues specific for IT1t in the CXCR4 co-crystal structure are indicated as dark blue squares with white text, specific interactions with peptide CVX-15 are shown with orange or dark gray squares with white text, whereas residues that interact with both IT1t and CVX-15 are indicated with bold black text. Data is obtained from primary literature, reviewed in two recent reviews (Roumen et al., 2012; Scholten et al., 2012a). Note that no data is included on ligands like metal chelators requiring modification of receptors to bind at all.

Figure 3

[^{125}I]-CXCL11 binding to membranes prepared from HEK293T cells transiently transfected with WT or selected CXCR3 receptor mutants. (**A**) [^{125}I]-CXCL11 homologous binding on WT (filled circles),

Molecular Pharmacology Fast Forward. Published on October 30, 2013 as DOI: 10.1124/mol.113.088633
This article has not been copyedited and formatted. The final version may differ from this version.

D112$^{2.63}$N (open upward triangles), D186$^{4.60}$N (filled diamonds), F131$^{3.32}$A (filled downward triangles), W109$^{2.60}$Q (open circles), and Y308$^{7.43}$A (filled upward triangles). (**B**) [^{125}I]-CXCL11 displacement by VUF11211 from CXCR3 WT (filled circles), D186$^{4.60}$N (open upward triangles), F131$^{3.32}$A (filled downward triangles), Y308$^{7.43}$A (filled downward triangles), and W2.60Q (open circles) by VUF11211 ligand. (**C**) [^{125}I]-CXCL11 displacement by NBI-74330 from CXCR3 WT (filled circles), D112$^{2.63}$N (open upward triangles), F131$^{3.32}$A (filled downward triangles), Y308$^{7.43}$A (filled downward triangles), and W109$^{2.60}$Q (open circles) by NBI-74330 ligand. Graphs represent grouped data from three or more experiments.

Figure 4

(**A and B)** Helical wheel diagrams are shown for a top view of the TM domains of CXCR3 with effects of mutations highlighted for (**A**) VUF11211 and (**B**) NBI-74330. Residues that show a 10 fold or more decrease in affinity upon mutation are indicated in red, and mutations that result in a decrease in affinity between 5 and 10 fold are indicated in orange. Residues that give a significant decrease (10 fold or more) in affinity when mutated together are shown in blue. Other residues that were mutated but did not give a significant change in affinity are colored gray. (**C and D**) 2D interaction plots are shown for VUF11211 (**C**) and NBI-74330 (**D**). Side chains of proposed interacting residues are shown in gray. Suggested receptor-ligand interactions are depicted as dashed lines. Polar and hydrogen bonding interactions are shown as blue dashed lines, whereas aromatic interactions are shown as gray dashed lines. The ligands are shown in green (VUF11211) and magenta (NBI-74330).

(E and F) Homology models of CXCR3 with the two ligands VUF11211 (**E**) and NBI-74330 (**F**). The ligands are shown in green (VUF11211) and magenta (NBI-74330), and the TM helices are shown in yellow. Side chains of proposed interacting residues are shown in gray. Hydrogen bonds/polar interactions are shown as dashed blue lines. For reasons of clarity, aromatic interactions are not shown in these panels (see panels **C and D**). Although VUF11211 is predicted to have a charge at the piperidine nitrogen (45%) or the trialkyl-nitrogen of the piperazine (43%), our data together with literature SAR, highly suggests that the piperidine-nitrogen engages in binding the D186$^{4.60}$ residue.

Molecular Pharmacology Fast Forward. Published on October 30, 2013 as DOI: 10.1124/mol.113.088633
This article has not been copyedited and formatted. The final version may differ from this version.

Figure 5

(**A**) Side-view of the homology model of CXCR3 with the binding modes for VUF11211 bridging both subpockets (TMS1 and TMS2; green) and NBI-74330 mainly in TMS1 (magenta). (**B**) Side-view of the CXCR4 receptor bound to the small ligand IT1t in TMS1 (cyan) and the peptide CVX-15 in TMS2 (orange), obtained by X-ray crystallography. (**C**) Side-view of the CCR5 receptor bound to the small ligand maraviroc in both TMS1 and TMS2, obtained by X-ray crystallography.

Molecular Pharmacology Fast Forward. Published on October 30, 2013 as DOI: 10.1124/mol.113.088633
This article has not been copyedited and formatted. The final version may differ from this version.

Tables

Table 1: Effects of mutation of of negatively charged residues in CXCR3 on protein expression, CXCL11 binding and affinities of small-molecule CXCR3 antagonists VUF11211 and NBI-74330

Region	**Construct**	**Expression**	**CXCL11**	**VUF11211**	**NBI-74330**
	CXCR3	*% WT± SEM*	*pK_d ± SEM*	*pIC_{50} ± SEM*	*pIC_{50} ± SEM*
	WT	100 ± 0	9.7 ± 0.1	7.8 ± 0.0	7.2 ± 0.1
N-term.	D46N	100 ± 3	9.3 ± 0.1	7.8 ± 0.1	7.2 ± 0.1
TM1	$D52^{1.31}N$	121 ± 8	9.6 ± 0.0	8.1 ± 0.1	7.5 ± 0.2
TM2	$D112^{2.63}N$	96 ± 6	9.6 ± 0.1	7.8 ± 0.1	6.1 ± 0.1*
TM4	$D186^{4.60}N$	68 ± 5	9.8 ± 0.0	6.8 ± 0.1*	7.7 ± 0.1
EL2	$D195^{45.42}N$	94 ± 8	9.8 ± 0.1	8.0 ± 0.3	7.1 ± 0.1
	$E196^{45.43}N$	93 ± 13	9.9 ± 0.1	7.7 ± 0.2	6.9 ± 0.2
TM6	$D278^{6.58}N$	84 ± 7	9.6 ± 0.1	7.9 ± 0.1	7.7 ± 0.1
	$D282^{6.62}N$	68 ± 4	N.D.	N.D.	N.D.
TM7	$E293^{7.28}N$	88 ± 8	9.3 ± 0.2	7.9 ± 0.1	7.4 ± 0.1
	$D297^{7.32}N$	110 ± 8	9.6 ± 0.2	8.1 ± 0.0	7.6 ± 0.1

Overview of both total receptor expression levels determined using whole cell-based ELISA, and affinity data for the three compounds. The latter was generated by performing [^{125}I]-CXCL11 radioligand displacement binding studies on membranes prepared from HEK293T cells transiently expressing CXCR3 WT or mutants. Shown values are averages ± SEM from at least three individual experiments. The Ballesteros-Weinstein residue numbers are indicated as superscript for residues in transmembrane (TM) helices, whereas the numbering scheme proposed by de Graaf and colleagues is used to enumerate residues in the second extracellular loop two (EL2) (Ballesteros and Weinstein, 1995; de Graaf et al., 2008).

N.D. the affinity could not be determined due to lack of specific [^{125}I]-CXCL11 binding.

$^{*}pIC_{50}$ value decreases with 10 fold or more.

$^{\#}$ pIC_{50} value decreases between 5 to 10 fold.

Molecular Pharmacology Fast Forward. Published on October 30, 2013 as DOI: 10.1124/mol.113.088633
This article has not been copyedited and formatted. The final version may differ from this version.

Table 2: Effects of mutation of aromatic and polar residues in CXCR3 on protein expression, CXCL11 binding and affinities of small molecule CXCR3 antagonists VUF11211 and NBI-74330

Region	Construct	Expression	CXCL11	VUF11211	NBI-74330
	CXCR3	*% WT±SEM*	*pK_d ± SEM*	*pIC_{50} ± SEM*	*pIC_{50} ± SEM*
	WT	100 ± 0	9.7 ± 0.1	7.8 ± 0.0	7.2 ± 0.1
TM1	$Y60^{1.39}A$	75 ± 7	9.8 ± 0.0	7.5 ± 0.2	6.9 ± 0.1
	$Y60^{1.39}F$	81 ± 9	9.5 ± 0.2	7.5 ± 0.1	7.3 ± 0.1
TM2	$W109^{2.60}Q$	81 ± 6	9.9 ± 0.1	≤5.0*	≤4.5*
TM3	$G128^{3.29}H$	80 ± 4	9.0 ± 0.1#	4.9 ± 0.4*	5.2 ± 0.0*
	$F131^{3.32}A$	74 ± 4	9.6 ± 0.2	6.5 ± 0.1*	6.3 ± 0.0*
	$F131^{3.32}H$	55 ± 8	9.6 ± 0.1	7.2 ± 0.2	7.0 ± 0.1
	$F135^{3.36}A$	106 ± 7	9.4 ± 0.1	7.5 ± 0.0	7.5 ± 0.1
TM6	$W268^{6.48}Q$	60 ± 4	9.8 ± 0.1	7.0 ± 0.1#	7.4 ± 0.1
	$Y271^{6.51}A$	41 ± 5	9.6 ± 0.1	6.8 ± 0.1*	6.4 ± 0.1#
TM7	$K300^{7.35}I$	94 ± 7	9.3 ± 0.1	7.7 ± 0.0	7.0 ± 0.1
	$S301^{7.36}A$	96 ± 1	9.2 ± 0.1	8.1 ± 0.1	6.9 ± 0.2
	$S304^{7.39}A$	111 ± 2	9.0 ± 0.1#	7.7 ± 0.1	7.3 ± 0.1
	$S304^{7.39}E$	91 ± 7	9.6 ± 0.1	7.6 ± 0.2	5.3 ± 0.4*
	$S304^{7.39}L$	95 ± 7	9.5 ± 0.1	6.5 ± 0.1*	5.9 ± 0.1*
	$Y308^{7.43}A$	75 ± 11	9.5 ± 0.1	6.9 ± 0.2#	5.7 ± 0.1*
	$Y308^{7.43}F$	95 ± 5	9.3 ± 0.1	7.3 ± 0.1	6.7 ± 0.1
Combi	$Y60^{1.39}F/S304^{7.39}A/Y308^{7.43}F$	96 ± 2	9.5 ± 0.0	6.8 ± 0.1*	6.7 ± 0.1

Overview of both total receptor expression determined using whole cell-based ELISA, and affinity data for the three compounds. pK_d and pIC_{50} values were obtained by performing [^{125}I]-CXCL11 radioligand displacement binding studies on membranes prepared from HEK293T cells transiently expressing CXCR3 WT or mutants. Shown values are averages ± SEM from at least three individual experiments.

* pIC_{50} value decreases with 10 fold or more.

pIC_{50} or pK_d values decrease between 5 to 10 fold.

Figure 1

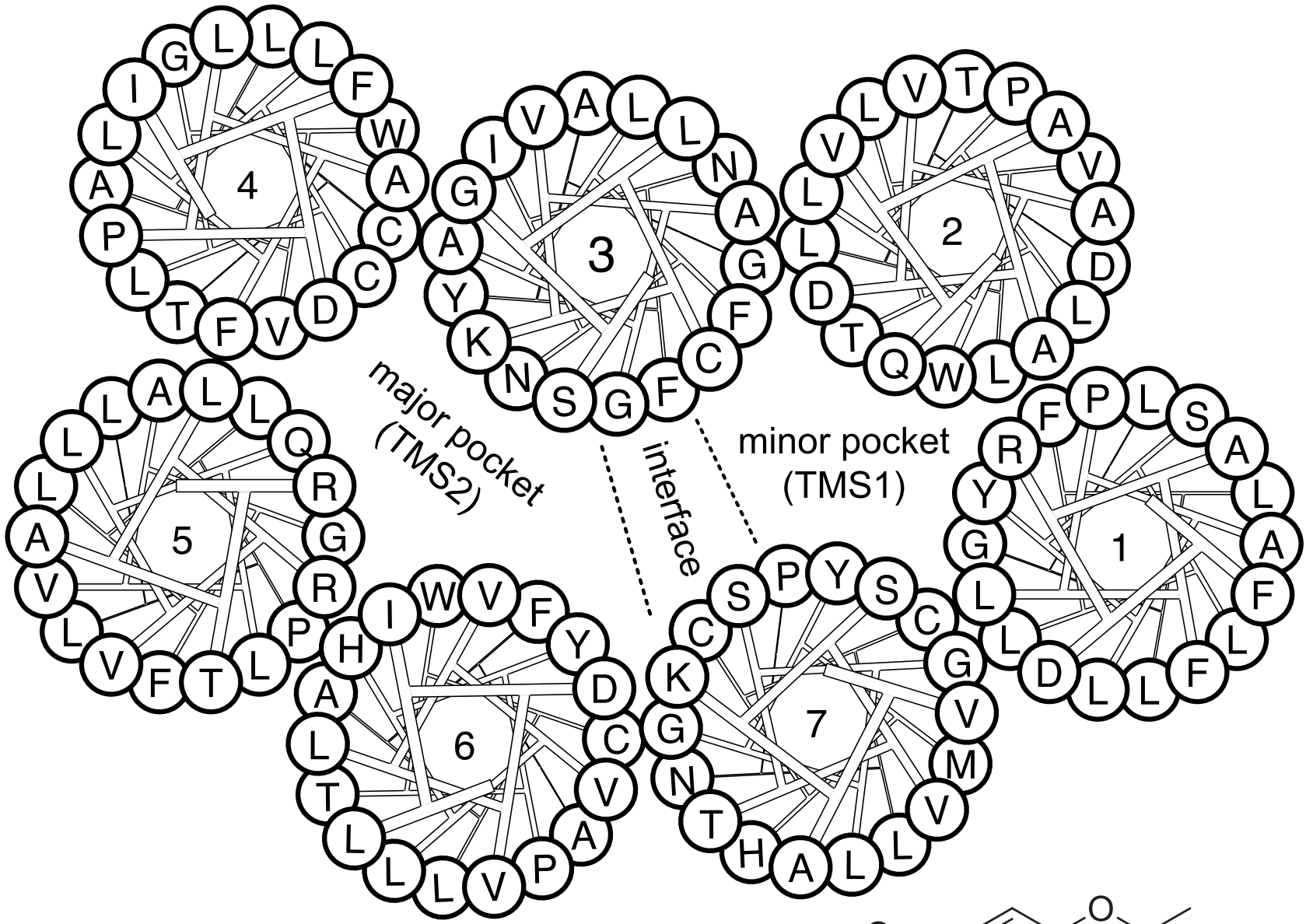

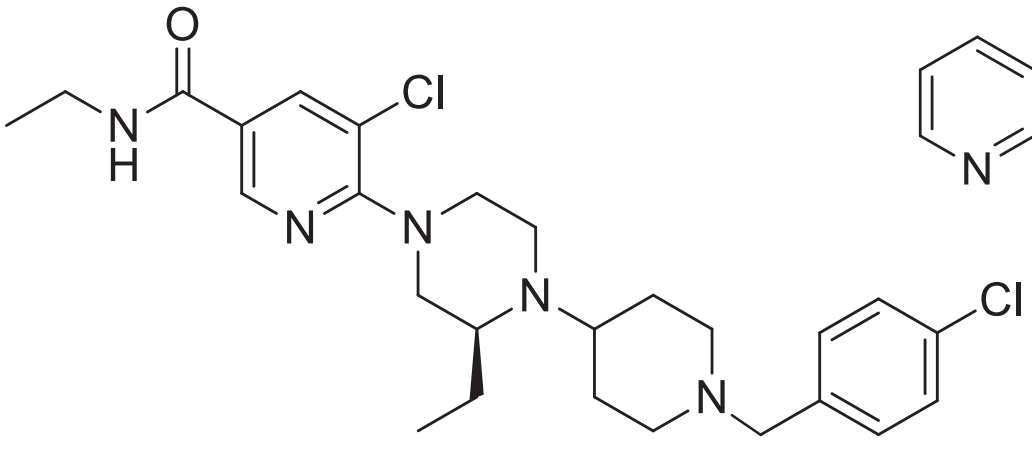

VUF11211

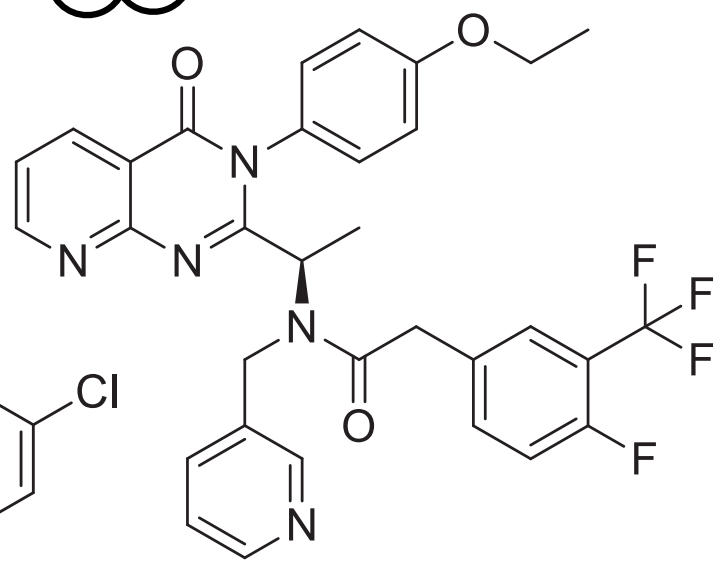

NBI-74330

Figure 2

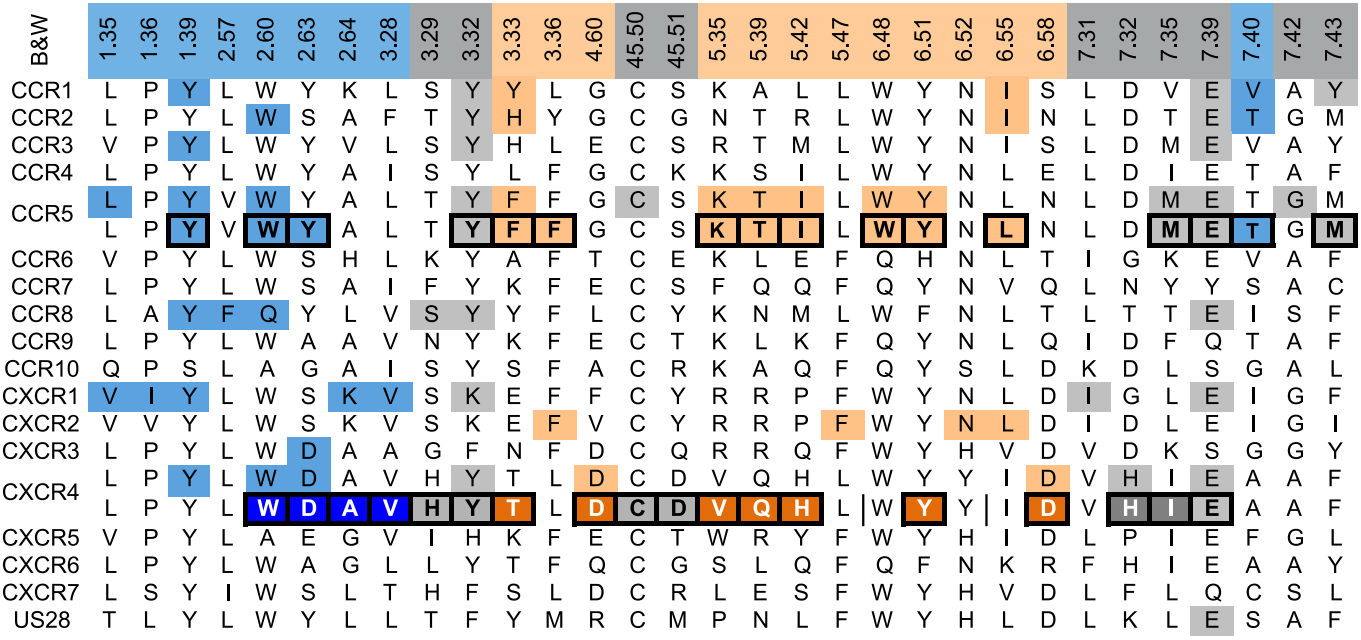
B&W
1.35 1.36 1.39 2.57 2.60 2.63 2.64 3.28 3.29 3.32 3.33 3.36 4.60 45.50 45.51 5.35 5.39 5.42 5.47 6.48 6.51 6.52 6.55 6.58 7.31 7.32 7.35 7.39 7.40 7.42 7.43
CCR1 L P Y L W Y K L S Y Y L G C S K A L L W Y N I S L D V E V A Y
CCR2 L P Y L W S A F T Y H Y G C G N T R L W Y N I N L D T E T G M
CCR3 V P Y L W Y V L S Y H L E C S R T M L W Y N I S L D M E V A Y
CCR4 L P Y L W Y A I S Y L F G C K K S I L W Y N L E L D I E T A F
CCR5 L P Y V W Y A L T Y F F G C S K T I L W Y N L N L D M E T G M
CCR5 L P Y V W Y A L T Y F F G C S K T I L W Y N L N L D M E T G M
CCR6 V P Y L W S H L K Y A F T C E K L E F Q H N L T I G K E V A F
CCR7 L P Y L W S A I F Y K F E C S F Q Q F Q Y N V Q L N Y Y S A C
CCR8 L A Y F Q Y L V S Y Y F L C Y K N M L W F N L T L T T E I S F
CCR9 L P Y L W A A V N Y K F E C T K L K F Q Y N L Q I D F Q T A F
CCR10 Q P S L A G A I S Y S F A C R K A Q F Q Y S L D K D L S G A L
CXCR1 V I Y L W S K V S K E F F C Y R R P F W Y N L D I G L E I G F
CXCR2 V V Y L W S K V S K E F V C Y R R P F W Y N L D I D L E I G I
CXCR3 L P Y L W D A A G F N F D C Q R R Q F W Y H V D V D K S G G Y
CXCR4 L P Y L W D A V H Y T L D C D V Q H L W Y Y I D V H I E A A F
CXCR4 L P Y L W D A V H Y T L D C D V Q H L W Y Y I D V H I E A A F
CXCR5 V P Y L A E G V I H K F E C T W R Y F W Y H I D L P I E F G L
CXCR6 L P Y L W A G L L Y T F Q C G S L Q F Q F N K R F H I E A A Y
CXCR7 L S Y I W S L T H F S L D C R L E S F W Y H V D L F L Q C S L
US28 T L Y L W Y L L T F Y M R C M P N L F W Y H L D L K L E S A F
TMS1 (minor)
interface
TMS2 (major)
Interaction point from crystal structure CCR5 (Maraviroc) or CXCR4 (IT1t / CVX15)
Specific contact with IT1t in CXCR4
Specific contact with CVX15 in CXCR4
contact with both IT1t and CVX15 in CXCR4

Figure 3

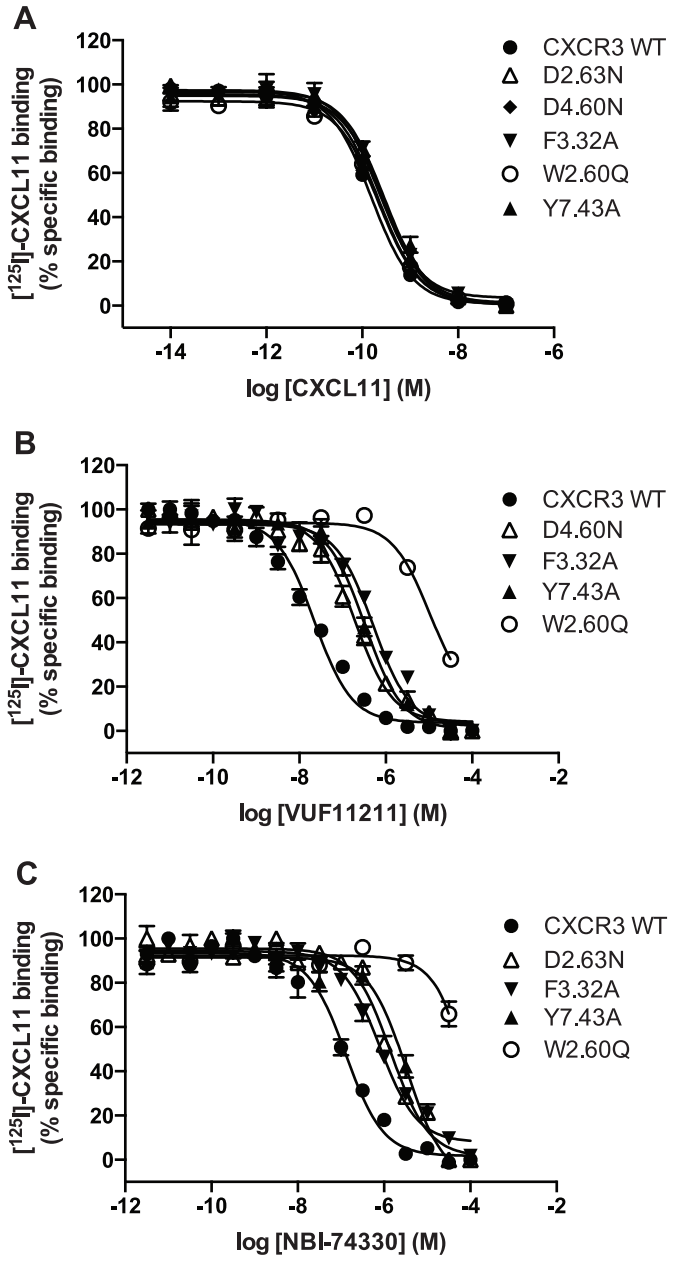
A
[125I]-CXCL11 binding (% specific binding)
120
100
80
60
40
20
0
-14
-12
-10
-8
-6
log [CXCL11] (M)
CXCR3 WT
D2.63N
D4.60N
F3.32A
W2.60Q
Y7.43A
B
[125I]-CXCL11 binding (% specific binding)
-12
-10
-8
-6
-4
-2
log [VUF11211] (M)
CXCR3 WT
D4.60N
F3.32A
Y7.43A
W2.60Q
C
[125I]-CXCL11 binding (% specific binding)
log [NBI-74330] (M)
CXCR3 WT
D2.63N
F3.32A
Y7.43A
W2.60Q

Figure 4

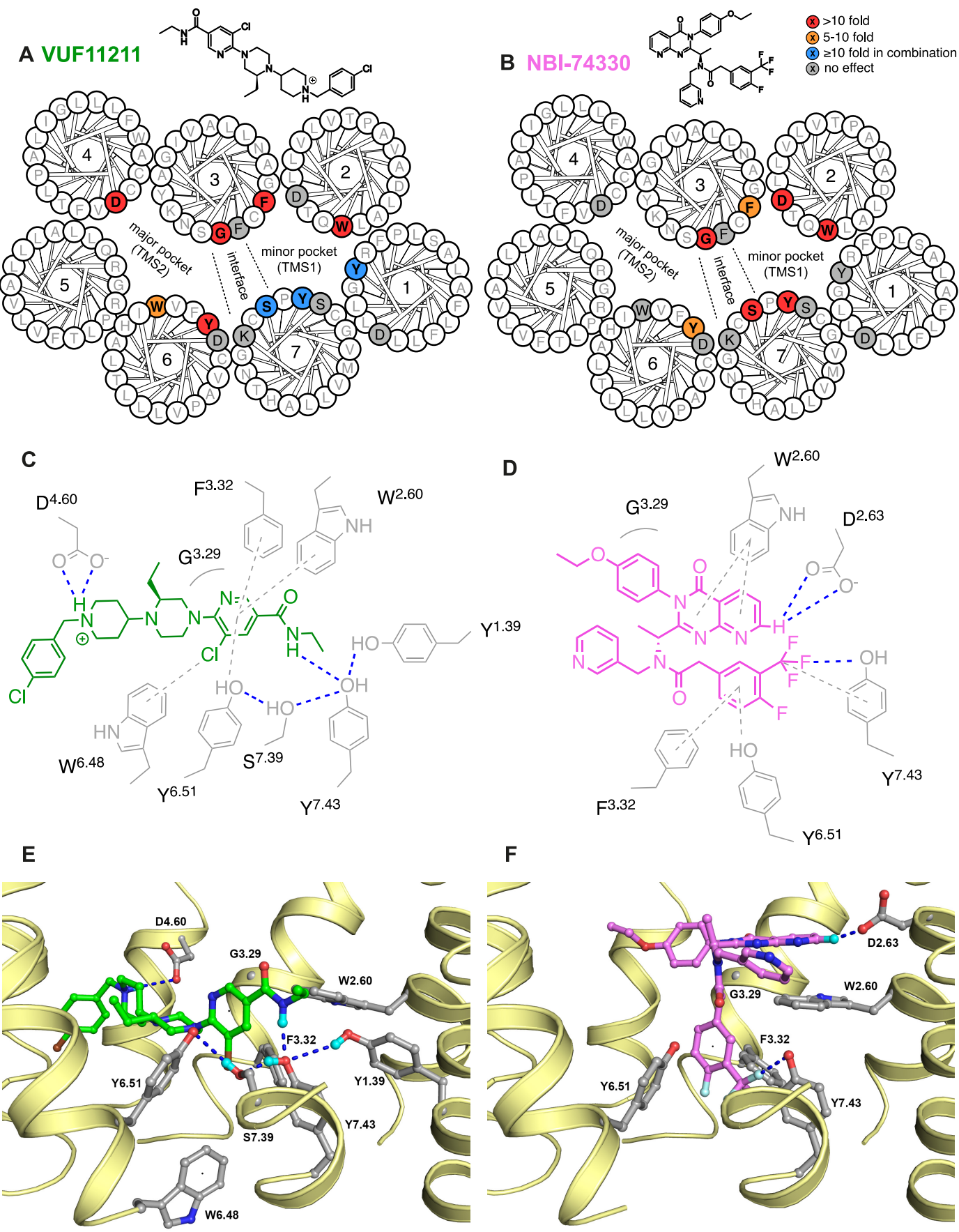
A VUF11211
B NBI-74330
>10 fold
5-10 fold
≥10 fold in combination
no effect
major pocket (TMS2)
interface
minor pocket (TMS1)
C
D
E
F
D4.60
F3.32
W2.60
G3.29
Y1.39
W6.48
S7.39
Y6.51
Y7.43
D2.63

Figure 5

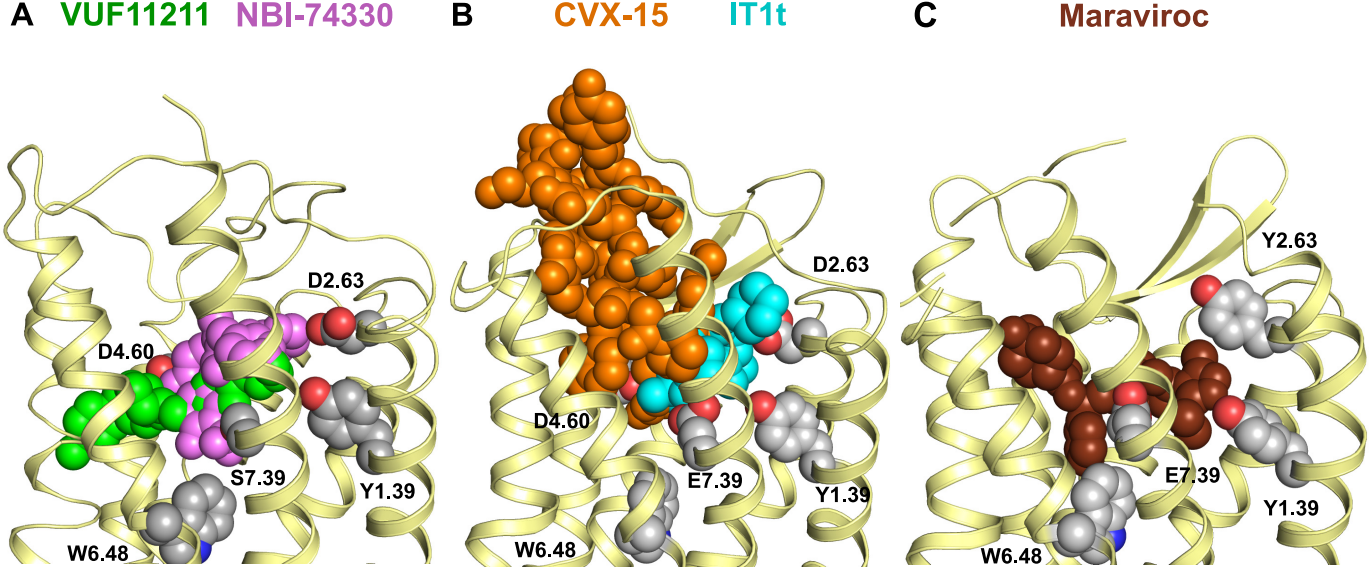
A
VUF11211
NBI-74330
D2.63
D4.60
S7.39
Y1.39
W6.48
B
CVX-15
IT1t
D2.63
D4.60
E7.39
Y1.39
W6.48
C
Maraviroc
Y2.63
E7.39
Y1.39
W6.48